



Differential cross section for w boson production as a function of transverse momentum in proton-antiproton collisions at $\sqrt{s} = 1.8$ TeV

V.M. Abazov, B. Abbott, Abdelmalek Abdesselam, M. Abolins, V. Abramov,
B.S. Acharya, D.L. Adams, M. Adams, S.N. Ahmed, G.D. Alexeev, et al.

► To cite this version:

V.M. Abazov, B. Abbott, Abdelmalek Abdesselam, M. Abolins, V. Abramov, et al.. Differential cross section for w boson production as a function of transverse momentum in proton-antiproton collisions at $\sqrt{s} = 1.8$ TeV. Physics Letters B, 2001, 513, pp.292-300. 10.1016/S0370-2693(01)00628-1 . in2p3-00010195

HAL Id: in2p3-00010195

<https://hal.in2p3.fr/in2p3-00010195>

Submitted on 3 Aug 2001

HAL is a multi-disciplinary open access archive for the deposit and dissemination of scientific research documents, whether they are published or not. The documents may come from teaching and research institutions in France or abroad, or from public or private research centers.

L'archive ouverte pluridisciplinaire **HAL**, est destinée au dépôt et à la diffusion de documents scientifiques de niveau recherche, publiés ou non, émanant des établissements d'enseignement et de recherche français ou étrangers, des laboratoires publics ou privés.

Differential Cross Section for W Boson Production as a Function of Transverse Momentum in $p\bar{p}$ Collisions at $\sqrt{s} = 1.8$ TeV

V.M. Abazov,²³ B. Abbott,⁵⁸ A. Abdesselam,¹¹ M. Abolins,⁵¹ V. Abramov,²⁶ B.S. Acharya,¹⁷ D.L. Adams,⁶⁰ M. Adams,³⁸ S.N. Ahmed,²¹ G.D. Alexeev,²³ G.A. Alves,² N. Amos,⁵⁰ E.W. Anderson,⁴³ M.M. Baarmand,⁵⁵ V.V. Babintsev,²⁶ L. Babukhadia,⁵⁵ T.C. Bacon,²⁸ A. Baden,⁴⁷ B. Baldin,³⁷ P.W. Balm,²⁰ S. Banerjee,¹⁷ E. Barberis,³⁰ P. Baringer,⁴⁴ J. Barreto,² J.F. Bartlett,³⁷ U. Bassler,¹² D. Bauer,²⁸ A. Bean,⁴⁴ M. Begel,⁵⁴ A. Belyaev,²⁵ S.B. Beri,¹⁵ G. Bernardi,¹² I. Bertram,²⁷ A. Besson,⁹ R. Beuselinck,²⁸ V.A. Bezzubov,²⁶ P.C. Bhat,³⁷ V. Bhatnagar,¹¹ M. Bhattacharjee,⁵⁵ G. Blazey,³⁹ S. Blessing,³⁵ A. Boehlein,³⁷ N.I. Bojko,²⁶ F. Borcherding,³⁷ K. Bos,²⁰ A. Brandt,⁶⁰ R. Breedon,³¹ G. Briskin,⁵⁹ R. Brock,⁵¹ G. Brooijmans,³⁷ A. Bross,³⁷ D. Buchholz,⁴⁰ M. Buehler,³⁸ V. Buescher,¹⁴ V.S. Burtovoi,²⁶ J.M. Butler,⁴⁸ F. Canelli,⁵⁴ W. Carvalho,³ D. Casey,⁵¹ Z. Casilum,⁵⁵ H. Castilla-Valdez,¹⁹ D. Chakraborty,⁵⁵ K.M. Chan,⁵⁴ S.V. Chekulaev,²⁶ D.K. Cho,⁵⁴ S. Choi,³⁴ S. Chopra,⁵⁶ J.H. Christenson,³⁷ M. Chung,³⁸ D. Claes,⁵² A.R. Clark,³⁰ J. Cochran,³⁴ L. Coney,⁴² B. Connolly,³⁵ W.E. Cooper,³⁷ D. Coppage,⁴⁴ M.A.C. Cummings,³⁹ D. Cutts,⁵⁹ G.A. Davis,⁵⁴ K. Davis,²⁹ K. De,⁶⁰ S.J. de Jong,²¹ K. Del Signore,⁵⁰ M. Demarteau,³⁷ R. Demina,⁴⁵ P. Demine,⁹ D. Denisov,³⁷ S.P. Denisov,²⁶ S. Desai,⁵⁵ H.T. Diehl,³⁷ M. Diesburg,³⁷ G. Di Loreto,⁵¹ S. Doulas,⁴⁹ P. Draper,⁶⁰ Y. Ducros,¹³ L.V. Dudko,²⁵ S. Duensing,²¹ L. Duflot,¹¹ S.R. Dugad,¹⁷ A. Dyshkant,²⁶ D. Edmunds,⁵¹ J. Ellison,³⁴ V.D. Elvira,³⁷ R. Engelmann,⁵⁵ S. Eno,⁴⁷ G. Eppley,⁶² P. Ermolov,²⁵ O.V. Eroshin,²⁶ J. Estrada,⁵⁴ H. Evans,⁵³ V.N. Evdokimov,²⁶ T. Fahland,³³ S. Feher,³⁷ D. Fein,²⁹ T. Ferbel,⁵⁴ F. Filthaut,²¹ H.E. Fisk,³⁷ Y. Fisyak,⁵⁶ E. Flattum,³⁷ F. Fleuret,³⁰ M. Fortner,³⁹ K.C. Frame,⁵¹ S. Fuess,³⁷ E. Gallas,³⁷ A.N. Galyaev,²⁶ M. Gao,⁵³ V. Gavrilov,²⁴ R.J. Genik II,²⁷ K. Genser,³⁷ C.E. Gerber,³⁸ Y. Gershtein,⁵⁹ R. Gilmartin,³⁵ G. Ginther,⁵⁴ B. Gómez,⁵ G. Gómez,⁴⁷ P.I. Goncharov,²⁶ J.L. González Solís,¹⁹ H. Gordon,⁵⁶ L.T. Goss,⁶¹ K. Gounder,³⁷ A. Goussiou,⁵⁵ N. Graf,⁵⁶ G. Graham,⁴⁷ P.D. Grannis,⁵⁵ J.A. Green,⁴³ H. Greenlee,³⁷ S. Grinstein,¹ L. Groer,⁵³ S. Grünendahl,³⁷ A. Gupta,¹⁷ S.N. Gurzhiev,²⁶ G. Gutierrez,³⁷ P. Gutierrez,⁵⁸ N.J. Hadley,⁴⁷ H. Haggerty,³⁷ S. Hagopian,³⁵ V. Hagopian,³⁵ R.E. Hall,³² P. Hanlet,⁴⁹ S. Hansen,³⁷ J.M. Hauptman,⁴³ C. Hays,⁵³ C. Hebert,⁴⁴ D. Hedin,³⁹ A.P. Heinson,³⁴ U. Heintz,⁴⁸ T. Heuring,³⁵ M.D. Hildreth,⁴²

R. Hirosky,⁶³ J.D. Hobbs,⁵⁵ B. Hoeneisen,⁸ Y. Huang,⁵⁰ R. Illingworth,²⁸ A.S. Ito,³⁷
M. Jaffré,¹¹ S. Jain,¹⁷ R. Jesik,⁴¹ K. Johns,²⁹ M. Johnson,³⁷ A. Jonckheere,³⁷
M. Jones,³⁶ H. Jöstlein,³⁷ A. Juste,³⁷ S. Kahn,⁵⁶ E. Kajfasz,¹⁰ A.M. Kalinin,²³
D. Karmanov,²⁵ D. Karmgard,⁴² R. Kehoe,⁵¹ A. Kharchilava,⁴² S.K. Kim,¹⁸ B. Klima,³⁷
B. Knuteson,³⁰ W. Ko,³¹ J.M. Kohli,¹⁵ A.V. Kostritskiy,²⁶ J. Kotcher,⁵⁶ A.V. Kotwal,⁵³
A.V. Kozelov,²⁶ E.A. Kozlovsky,²⁶ J. Krane,⁴³ M.R. Krishnaswamy,¹⁷ P. Krikova,⁶
S. Krzywdzinski,³⁷ M. Kubantsev,⁴⁵ S. Kuleshov,²⁴ Y. Kulik,⁵⁵ S. Kunori,⁴⁷ A. Kupco,⁷
V.E. Kuznetsov,³⁴ G. Landsberg,⁵⁹ A. Leflat,²⁵ C. Leggett,³⁰ F. Lehner,³⁷ J. Li,⁶⁰ Q.Z. Li,³⁷
J.G.R. Lima,³ D. Lincoln,³⁷ S.L. Linn,³⁵ J. Linnemann,⁵¹ R. Lipton,³⁷ A. Lucotte,⁹
L. Lueking,³⁷ C. Lundstedt,⁵² C. Luo,⁴¹ A.K.A. Maciel,³⁹ R.J. Madaras,³⁰ V.L. Malyshev,²³
V. Manankov,²⁵ H.S. Mao,⁴ T. Marshall,⁴¹ M.I. Martin,³⁷ R.D. Martin,³⁸ K.M. Mauritz,⁴³
B. May,⁴⁰ A.A. Mayorov,⁴¹ R. McCarthy,⁵⁵ J. McDonald,³⁵ T. McMahon,⁵⁷ H.L. Melanson,³⁷
M. Merkin,²⁵ K.W. Merritt,³⁷ C. Miao,⁵⁹ H. Miettinen,⁶² D. Mihalcea,⁵⁸ C.S. Mishra,³⁷
N. Mokhov,³⁷ N.K. Mondal,¹⁷ H.E. Montgomery,³⁷ R.W. Moore,⁵¹ M. Mostafa,¹ H. da Motta,²
E. Nagy,¹⁰ F. Nang,²⁹ M. Narain,⁴⁸ V.S. Narasimham,¹⁷ H.A. Neal,⁵⁰ J.P. Negret,⁵
S. Negroni,¹⁰ T. Nunnemann,³⁷ D. O'Neil,⁵¹ V. Oguri,³ B. Olivier,¹² N. Oshima,³⁷
P. Padley,⁶² L.J. Pan,⁴⁰ K. Papageorgiou,²⁸ A. Para,³⁷ N. Parashar,⁴⁹ R. Partridge,⁵⁹
N. Parua,⁵⁵ M. Paterno,⁵⁴ A. Patwa,⁵⁵ B. Pawlik,²² J. Perkins,⁶⁰ M. Peters,³⁶
O. Peters,²⁰ P. Pétroff,¹¹ R. Piegaia,¹ H. Piekarz,³⁵ B.G. Pope,⁵¹ E. Popkov,⁴⁸
H.B. Prosper,³⁵ S. Protopopescu,⁵⁶ J. Qian,⁵⁰ R. Raja,³⁷ S. Rajagopalan,⁵⁶ E. Ramberg,³⁷
P.A. Rapidis,³⁷ N.W. Reay,⁴⁵ S. Reucroft,⁴⁹ J. Rha,³⁴ M. Ridel,¹¹ M. Rijssenbeek,⁵⁵
T. Rockwell,⁵¹ M. Roco,³⁷ P. Rubinov,³⁷ R. Ruchti,⁴² J. Rutherford,²⁹ B.M. Sabirov,²³
A. Santoro,² L. Sawyer,⁴⁶ R.D. Schamberger,⁵⁵ H. Schellman,⁴⁰ A. Schwartzman,¹ N. Sen,⁶²
E. Shabalina,²⁵ R.K. Shivpuri,¹⁶ D. Shpakov,⁴⁹ M. Shupe,²⁹ R.A. Sidwell,⁴⁵ V. Simak,⁷
H. Singh,³⁴ J.B. Singh,¹⁵ V. Sirotenko,³⁷ P. Slattery,⁵⁴ E. Smith,⁵⁸ R.P. Smith,³⁷
R. Snihur,⁴⁰ G.R. Snow,⁵² J. Snow,⁵⁷ S. Snyder,⁵⁶ J. Solomon,³⁸ V. Sorín,¹
M. Sosebee,⁶⁰ N. Sotnikova,²⁵ K. Soustruznik,⁶ M. Souza,² N.R. Stanton,⁴⁵ G. Steinbrück,⁵³
R.W. Stephens,⁶⁰ F. Stichelbaut,⁵⁶ D. Stoker,³³ V. Stolin,²⁴ D.A. Stoyanova,²⁶ M. Strauss,⁵⁸
M. Strovink,³⁰ L. Stutte,³⁷ A. Sznajder,³ W. Taylor,⁵⁵ S. Tentindo-Repond,³⁵ S.M. Tripathi,³¹
T.G. Trippe,³⁰ A.S. Turcot,⁵⁶ P.M. Tuts,⁵³ P. van Gemmeren,³⁷ V. Vaniev,²⁶ R. Van Kooten,⁴¹
N. Varelas,³⁸ L.S. Vertogradov,²³ A.A. Volkov,²⁶ A.P. Vorobieff,²⁶ H.D. Wahl,³⁵ H. Wang,⁴⁰
Z.-M. Wang,⁵⁵ J. Warchol,⁴² G. Watts,⁶⁴ M. Wayne,⁴² H. Weerts,⁵¹ A. White,⁶⁰ J.T. White,⁶¹
D. Whiteson,³⁰ J.A. Wightman,⁴³ D.A. Wijngaarden,²¹ S. Willis,³⁹ S.J. Wimpenny,³⁴
J. Womersley,³⁷ D.R. Wood,⁴⁹ R. Yamada,³⁷ P. Yamin,⁵⁶ T. Yasuda,³⁷ Y.A. Yatsunenko,²³
K. Yip,⁵⁶ S. Youssef,³⁵ J. Yu,³⁷ Z. Yu,⁴⁰ M. Zanabria,⁵ H. Zheng,⁴² Z. Zhou,⁴³

M. Zielinski,⁵⁴ D. Ziemińska,⁴¹ A. Ziemiński,⁴¹ V. Zutshi,⁵⁴ E.G. Zverev,²⁵ and A. Zyberstejn¹³

(DØ Collaboration)

¹*Universidad de Buenos Aires, Buenos Aires, Argentina*

²*LAFEX, Centro Brasileiro de Pesquisas Físicas, Rio de Janeiro, Brazil*

³*Universidade do Estado do Rio de Janeiro, Rio de Janeiro, Brazil*

⁴*Institute of High Energy Physics, Beijing, People's Republic of China*

⁵*Universidad de los Andes, Bogotá, Colombia*

⁶*Charles University, Center for Particle Physics, Prague, Czech Republic*

⁷*Institute of Physics, Academy of Sciences, Center for Particle Physics, Prague, Czech Republic*

⁸*Universidad San Francisco de Quito, Quito, Ecuador*

⁹*Institut des Sciences Nucléaires, IN2P3-CNRS, Université de Grenoble 1, Grenoble, France*

¹⁰*CPPM, IN2P3-CNRS, Université de la Méditerranée, Marseille, France*

¹¹*Laboratoire de l'Accélérateur Linéaire, IN2P3-CNRS, Orsay, France*

¹²*LPNHE, Universités Paris VI and VII, IN2P3-CNRS, Paris, France*

¹³*DAPNIA/Service de Physique des Particules, CEA, Saclay, France*

¹⁴*Universität Mainz, Institut für Physik, Mainz, Germany*

¹⁵*Panjab University, Chandigarh, India*

¹⁶*Delhi University, Delhi, India*

¹⁷*Tata Institute of Fundamental Research, Mumbai, India*

¹⁸*Seoul National University, Seoul, Korea*

¹⁹*CINVESTAV, Mexico City, Mexico*

²⁰*FOM-Institute NIKHEF and University of Amsterdam/NIKHEF, Amsterdam, The Netherlands*

²¹*University of Nijmegen/NIKHEF, Nijmegen, The Netherlands*

²²*Institute of Nuclear Physics, Kraków, Poland*

²³*Joint Institute for Nuclear Research, Dubna, Russia*

²⁴*Institute for Theoretical and Experimental Physics, Moscow, Russia*

²⁵*Moscow State University, Moscow, Russia*

²⁶*Institute for High Energy Physics, Protvino, Russia*

²⁷*Lancaster University, Lancaster, United Kingdom*

²⁸*Imperial College, London, United Kingdom*

²⁹*University of Arizona, Tucson, Arizona 85721*

- ³⁰*Lawrence Berkeley National Laboratory and University of California, Berkeley, California 94720*
- ³¹*University of California, Davis, California 95616*
- ³²*California State University, Fresno, California 93740*
- ³³*University of California, Irvine, California 92697*
- ³⁴*University of California, Riverside, California 92521*
- ³⁵*Florida State University, Tallahassee, Florida 32306*
- ³⁶*University of Hawaii, Honolulu, Hawaii 96822*
- ³⁷*Fermi National Accelerator Laboratory, Batavia, Illinois 60510*
- ³⁸*University of Illinois at Chicago, Chicago, Illinois 60607*
- ³⁹*Northern Illinois University, DeKalb, Illinois 60115*
- ⁴⁰*Northwestern University, Evanston, Illinois 60208*
- ⁴¹*Indiana University, Bloomington, Indiana 47405*
- ⁴²*University of Notre Dame, Notre Dame, Indiana 46556*
- ⁴³*Iowa State University, Ames, Iowa 50011*
- ⁴⁴*University of Kansas, Lawrence, Kansas 66045*
- ⁴⁵*Kansas State University, Manhattan, Kansas 66506*
- ⁴⁶*Louisiana Tech University, Ruston, Louisiana 71272*
- ⁴⁷*University of Maryland, College Park, Maryland 20742*
- ⁴⁸*Boston University, Boston, Massachusetts 02215*
- ⁴⁹*Northeastern University, Boston, Massachusetts 02115*
- ⁵⁰*University of Michigan, Ann Arbor, Michigan 48109*
- ⁵¹*Michigan State University, East Lansing, Michigan 48824*
- ⁵²*University of Nebraska, Lincoln, Nebraska 68588*
- ⁵³*Columbia University, New York, New York 10027*
- ⁵⁴*University of Rochester, Rochester, New York 14627*
- ⁵⁵*State University of New York, Stony Brook, New York 11794*
- ⁵⁶*Brookhaven National Laboratory, Upton, New York 11973*
- ⁵⁷*Langston University, Langston, Oklahoma 73050*
- ⁵⁸*University of Oklahoma, Norman, Oklahoma 73019*
- ⁵⁹*Brown University, Providence, Rhode Island 02912*
- ⁶⁰*University of Texas, Arlington, Texas 76019*
- ⁶¹*Texas A&M University, College Station, Texas 77843*
- ⁶²*Rice University, Houston, Texas 77005*
- ⁶³*University of Virginia, Charlottesville, Virginia 22901*
- ⁶⁴*University of Washington, Seattle, Washington 98195*

Abstract

We report a measurement of the differential cross section for W boson production as a function of its transverse momentum in proton-antiproton collisions at $\sqrt{s} = 1.8$ TeV. The data were collected by the D \emptyset experiment at the Fermilab Tevatron Collider during 1994–1995 and correspond to an integrated luminosity of 85 pb^{-1} . The results are in good agreement with quantum chromodynamics over the entire range of transverse momentum.

Key words: PACS numbers 12.35.Qk,14.70.Fm,12.38.Qk

Measurement of the differential cross section for W boson production provides an important test of our understanding of quantum chromodynamics (QCD). Its implications range from impact on the precision determination of the W boson mass to background estimates for new physics phenomena. Data from the production of W and Z bosons at hadron colliders also provide bounds on parametrizations used to describe the nonperturbative regime of QCD processes.

The production of W bosons at the Fermilab Tevatron proton-antiproton collider proceeds predominantly via quark-antiquark annihilation. In the QCD description of the production mechanism, the W boson acquires transverse momentum by recoiling against additional gluons or quarks, which at first order originate from the processes $qq' \rightarrow Wg$ and $qg \rightarrow Wq'$. When the transverse momentum (p_T^W) and the invariant mass (M_W) of the W boson are of the same order, the production rate can be calculated perturbatively order by order in the strong coupling constant α_s [1]. For $p_T^W \ll M_W$, the calculation is dominated by large logarithms $\approx \alpha_s \ln(M_W/p_T^W)^2$, which are related to the presence of soft and collinear gluon radiation. Therefore, at sufficiently small p_T^W , fixed-order perturbation theory breaks down and the logarithms must be resummed [2]. The resummation can be carried out in transverse momentum (p_T) space [3] or in impact parameter (b) space [4] via a Fourier transform. Differences between the two formalisms are discussed in Ref. [5].

Although resummation extends the perturbative calculation to lower values of p_T^W , a more fundamental barrier is encountered when p_T^W approaches Λ_{QCD} , the scale characterizing QCD processes. The strong coupling constant α_s becomes large and the perturbative calculation is no longer reliable. The problem is circumvented by using a cutoff value and by introducing an additional function that parametrizes the nonperturbative effects [6,7]. The specific form of this function and the particular choices for the nonperturbative parameters have to be adjusted to give the best possible description of the data.

We report a new measurement [8] of the inclusive differential cross section for W boson production in the electron channel as a function of transverse momentum. We use 85 pb^{-1} of data recorded with the DØ detector during the 1994–1995 run of the Fermilab Tevatron $p\bar{p}$ collider. We have a ten-fold increase in the number of W boson candidates with respect to our previous measurement [9], reflecting the larger data set and an increase in electron rapidity coverage. An improved electron identification technique reduces the background for central rapidities and high p_T^W by a factor of five compared to Ref. [9], and keeps the background contamination at a low level for large rapidities. Furthermore, corrections for detector resolution now enable direct comparison with theory.

Electrons are detected in an electromagnetic (EM) calorimeter which has a fractional energy resolution of $\approx 15\%/\sqrt{E(\text{GeV})}$ and a segmentation of $\Delta\eta \times \Delta\phi = 0.1 \times 0.1$ in pseudorapidity (η) and azimuth (ϕ). The DØ detector and the methods used to select $W \rightarrow e\nu$ events are discussed in detail in Refs. [10] and [11] respectively. Below, we briefly describe the main selection requirements.

Electron candidates are identified as isolated clusters of energy in the EM calorimeter that have a matching track in one of the drift chambers. In event reconstruction, electron identification is based on a likelihood technique [12]. The electron likelihood is constructed from: (i) a χ^2 based on a covariance matrix that determines the consistency of the cluster in the calorimeter with the expected shape of an electron shower, (ii) the “electromagnetic energy fraction,” defined as the ratio of the portion of the energy of the cluster found in the EM calorimeter to its total energy, (iii) a measure of the consistency between the track position and the centroid of the cluster, and (iv) the ionization energy loss along the track. To a good approximation, these four variables are independent of each other. Electron candidates are accepted either in the central region, $|\eta_{\text{det}}| \leq 1.1$, or in the forward region, $1.5 \leq |\eta_{\text{det}}| \leq 2.5$, where η_{det} refers to the value of η obtained by assuming that the particle originates from the geometrical center of the DØ detector.

Neutrinos do not interact in the detector and thereby create an apparent momentum imbalance. For each event, the missing transverse energy (\cancel{E}_T), obtained from the vectorial sum of the transverse energy of all calorimeter cells, is attributed to the neutrino.

Candidates for the $W \rightarrow e\nu$ event sample are required to have an electron with $E_T > 25 \text{ GeV}$ and $\cancel{E}_T > 25 \text{ GeV}$. Additionally, events containing a second electron are rejected if the dielectron invariant mass M_{ee} is close to that of the Z boson ($75 \text{ GeV}/c^2 < M_{ee} < 105 \text{ GeV}/c^2$). A total of 50,486 events passes this selection.

A major source of background stems from jets and direct photons passing our electron selection criteria. A multijet event can be misinterpreted as a $W \rightarrow e\nu$ decay if one of the jets mimics an electron and there is sufficient mismeasurement of energy to produce significant \cancel{E}_T . The fraction of background events due to multijet, b quark, and direct-photon sources, also referred to as QCD background, is calculated by studying the electron likelihood in both a background sample and a signal sample, as described in Ref. [13]. The total QCD background in the data sample is 2%; its shape is determined by repeating the background calculation for each p_T^W bin.

Other sources of background in the $W \rightarrow e\nu$ sample are $W \rightarrow \tau\nu$, $Z \rightarrow ee$, and $t\bar{t}$ events. The process $W \rightarrow \tau\nu \rightarrow e\nu\nu\nu$ is indistinguishable from the signal on an event-by-event basis. To estimate this background, $W \rightarrow \tau\nu$ events are generated with the same W boson production and decay model used in the calculation of the acceptance (see below), and the τ leptons are forced to decay to electrons. Since the three-body decay of the τ leads to a very soft electron p_T spectrum compared to that from $W \rightarrow e\nu$ events, the kinematic requirements keep this background to a moderate 2%. This is accounted for by making a correction to the acceptance for W bosons [13]. A $Z \rightarrow ee$ event can be misidentified when one of the two electrons escapes detection or is poorly reconstructed in the detector and thereby simulates the presence of a neutrino. This background (0.5%) is estimated by applying the selection criteria to a sample of Monte Carlo $Z \rightarrow ee$ events that were generated with ISAJET [14], processed through a GEANT-based [15] simulation of the DØ detector, and overlaid with events from random $p\bar{p}$ crossings that follow the luminosity profile of the data. The background from top quarks decaying to W bosons (0.1%) is estimated using HERWIG [16] Monte Carlo $t\bar{t}$ events and GEANT detector simulation.

Trigger and selection efficiencies are determined using $Z \rightarrow ee$ data in which one of the electrons satisfies the trigger and selection criteria, and the second electron provides an unbiased sample to measure the efficiencies. Due to the limited statistics of the $Z \rightarrow ee$ data sample, we determine the shape of the efficiency as a function of transverse momentum using $Z \rightarrow ee$ events generated with HERWIG, processed with a GEANT detector simulation, and overlaid with randomly selected minimum-bias $p\bar{p}$ collisions. This procedure models the effects of the underlying event and of jet activity on the selection of electrons. The efficiency for both the electron identification and the trigger requirements is $(55.3 \pm 2.2)\%$.

The data are corrected for kinematic and geometric acceptance and detector resolution, as determined from a Monte Carlo program originally developed for measuring the mass of the W boson [17]. The method is described in detail in Ref. [18]. The program first generates W bosons with η and p_T^W values chosen randomly from a double differential cross section $d^2\sigma/dp_T^W d\eta$ provided as

input. The response of the detector and the effects of geometric and kinematic selection criteria are introduced at the next stage. For the present analysis, the input $d^2\sigma/dp_T^W d\eta$ distribution is obtained using the iterative unfolding method described in Ref. [19]. The uncertainty due to this input distribution is evaluated by using an initial distribution uniform in p_T^W and η . The systematic smearing uncertainty is determined by varying the detector resolution parameters by ± 1 standard deviation from the nominal values. The total correction for kinematic and geometric acceptance and detector resolution for $W \rightarrow e\nu$ events is $(47.6 \pm 0.3)\%$.

The results for $d\sigma(W \rightarrow e\nu)/dp_T^W$, corrected for detector acceptance and resolution, are shown in Table 1 and plotted in Fig. 1, where the data are compared to the combined QCD perturbative and resummed calculation in b -space, computed with published values of the nonperturbative parameters [6]. The error bars on the data points correspond to their statistical uncertainties. The fractional systematic uncertainty is shown as a band in the lower portion of the plot. The largest contributions to the systematic error are from uncertainties in the hadronic energy scale and resolution, the selection efficiency, and the background (in the high p_T^W region). An additional normalization uncertainty of $\pm 4.4\%$ from the integrated luminosity is not included in any of the plots nor in the table. The data are normalized to the measured $W \rightarrow e\nu$ cross section (2310 pb [13]). The points are plotted at the values of p_T^W where the predicted function equals its mean over the bin [20].

Figure 2 shows a comparison of the differential cross section for W boson production, assuming $B(W \rightarrow e\nu) = 0.111$, to the fixed-order perturbative calculation and to three different resummation calculations in the low p_T^W region. The parametrizations of the nonperturbative region are from Arnold-Kauffman [5] and Ladinsky-Yuan [6] in b -space, and Ellis-Veseli [7] in p_T -space. The disagreement between the data and the fixed-order prediction at low values of p_T^W confirms the presence of contributions from soft gluon emission, which are accounted for in the resummation formalisms. The fractional differences (Data – Theory)/Theory are also shown in Fig. 2 for each of the three resummation predictions. Although the χ^2 for the Ellis-Veseli and Arnold-Kauffman prescriptions are not as good as for Ladinsky-Yuan, the flexibility in parameter space and in the form of the nonperturbative function in all three resummed models is such that a good description of our measurement can be achieved [18,21].

Figure 3 shows the differential cross section for W boson production in the intermediate and high p_T^W regions. The calculation by Ladinsky-Yuan [6] specifies a matching prescription which provides a smooth transition between the resummed and the fixed-order perturbative results to $\mathcal{O}(\alpha_s^2)$. The p_T -space result by Ellis-Veseli [7] contains only the $\mathcal{O}(\alpha_s)$ finite part and an $\mathcal{O}(\alpha_s^2)$ Sudakov form factor. Hence, there is still a residual unmatched higher-order effect

present in $d\sigma/dp_T^W$ in the large p_T^W region, where the cancellation of the different parts is quite delicate. The b -space prediction by Arnold-Kauffman [5] uses the matched result below $p_T^W = 50$ GeV/ c and the pure conventional perturbative $\mathcal{O}(\alpha_s^2)$ result above. We observe good agreement with the theoretical predictions for intermediate and high values of p_T^W , which probes effects of fixed-order QCD.

In summary, we have used data taken with the DØ detector in $p\bar{p}$ collisions at $\sqrt{s} = 1.8$ TeV to measure the cross section for $W \rightarrow e\nu$ events as a function of p_T^W . The combined QCD perturbative and resummed predictions are in agreement with the fully corrected p_T spectrum of W boson production in the kinematic range of the measurement.

We thank the staffs at Fermilab and collaborating institutions, and acknowledge support from the Department of Energy and National Science Foundation (USA), Commissariat à L’Energie Atomique and CNRS/Institut National de Physique Nucléaire et de Physique des Particules (France), Ministry for Science and Technology and Ministry for Atomic Energy (Russia), CAPES and CNPq (Brazil), Departments of Atomic Energy and Science and Education (India), Colciencias (Colombia), CONACyT (Mexico), Ministry of Education and KOSEF (Korea), CONICET and UBACyT (Argentina), The Foundation for Fundamental Research on Matter (The Netherlands), PPARC (United Kingdom), A.P. Sloan Foundation, and the A. von Humboldt Foundation.

References

- [1] P. B. Arnold and M. H. Reno, Nucl. Phys. **B319**, 37 (1989).
- [2] J. C. Collins, D. E. Soper, and G. Sterman, Nucl. Phys. **B250**, 199 (1985).
- [3] Y. L. Dokshitzer, D. Diakonov, and S. I. Troian, Phys. Lett. B **79**, 269 (1978); Phys. Rep. **58**, 269 (1980).
- [4] G. Parisi and R. Petronzio, Nucl. Phys. **B154**, 427 (1979).
- [5] P. B. Arnold and R. P. Kauffman, Nucl. Phys. **B349**, 381 (1991).
- [6] G. A. Ladinsky and C. P. Yuan, Phys. Rev. D **50**, 4239 (1994).
- [7] R. K. Ellis and S. Veseli, Nucl. Phys. **B511**, 649 (1998).
- [8] M. Mostafá, Ph.D. thesis, Instituto Balseiro, Univ. Nac. de Cuyo, Argentina, 2000 (in preparation).
- [9] B. Abbott *et al.*, (DØ Collaboration), Phys. Rev. Lett. **80**, 5498 (1998).
- [10] S. Abachi *et al.*, (DØ Collaboration), Nucl. Instrum. Methods A **338**, 185 (1994).

- [11] B. Abbott *et al.*, (DØ Collaboration), [hep-ex/0009034](#), submitted to Phys. Rev. D.
- [12] B. Abbott *et al.*, (DØ Collaboration), Phys. Rev. D **58**, 052001 (1998).
- [13] B. Abbott *et al.*, (DØ Collaboration), Phys. Rev. D **61**, 072001 (2000).
- [14] H. Baer, F. E. Paige, S. D. Protopopescu, and X. Tata, [hep-ph/0001086](#) (unpublished).
- [15] F. Carminati, CERN Program Library Long Write-up W5013, 1993 (unpublished).
- [16] G. Marchesini *et al.*, Comput. Phys. Commun. **67**, 465 (1992).
- [17] B. Abbott *et al.*, (DØ Collaboration), Phys. Rev. D **58**, 092003 (1998).
- [18] B. Abbott *et al.*, (DØ Collaboration), Phys. Rev. D **61**, 032004 (2000).
- [19] L. Lindemann and G. Zech, Nucl. Instrum. Methods A **354**, 516 (1995).
- [20] G. D. Lafferty and T. R. Wyatt, Nucl. Instrum. Methods A **355**, 541 (1995).
- [21] R. K. Ellis, D. A. Ross, and S. Veseli, Nucl. Phys. **B503**, 309 (1997).

Table 1

Summary of the measurement of the p_T distribution of the W boson. The nominal p_T^W is where the predicted function equals its mean value over the bin. The quantity $d\sigma(W \rightarrow e\nu)/dp_T^W$ corresponds to the differential cross section in each bin of p_T^W for $W \rightarrow e\nu$ production. Systematic uncertainties do not include an overall 4.4% normalization uncertainty in integrated luminosity.

p_T^W	p_T^W bin	$\frac{d\sigma(W \rightarrow e\nu)}{dp_T^W}$	Statistical uncertainty	Systematic uncertainty
GeV/ c	GeV/ c	pb/(GeV/ c)	pb/(GeV/ c)	pb/(GeV/ c)
0.92	0–2	109.37	± 4.60	± 10.64
3.40	2–4	205.91	± 6.84	± 22.80
4.97	4–6	171.28	± 5.64	± 9.16
6.98	6–8	133.62	± 4.65	± 9.81
8.98	8–10	103.30	± 4.03	± 7.17
10.98	10–12	77.58	± 3.47	± 7.15
12.98	12–14	63.66	± 3.21	± 4.18
14.98	14–16	47.88	± 2.77	± 4.03
16.98	16–18	37.72	± 2.43	± 2.50
18.98	18–20	30.65	± 2.21	± 1.60
22.40	20–25	22.02	± 1.23	± 1.11
27.41	25–30	13.94	± 0.93	± 0.98
32.42	30–35	9.47	± 0.73	± 0.79
37.42	35–40	6.84	± 0.63	± 0.52
44.70	40–50	3.95	± 0.36	± 0.31
54.72	50–60	1.81	± 0.24	± 0.23
64.77	60–70	1.15	± 0.21	± 0.25
74.79	70–80	0.75	± 0.18	± 0.21
89.21	80–100	0.313	± 0.059	± 0.091
109.27	100–120	0.084	± 0.029	± 0.018
137.40	120–160	0.044	± 0.012	± 0.014
177.64	160–200	0.0077	± 0.0054	± 0.0045

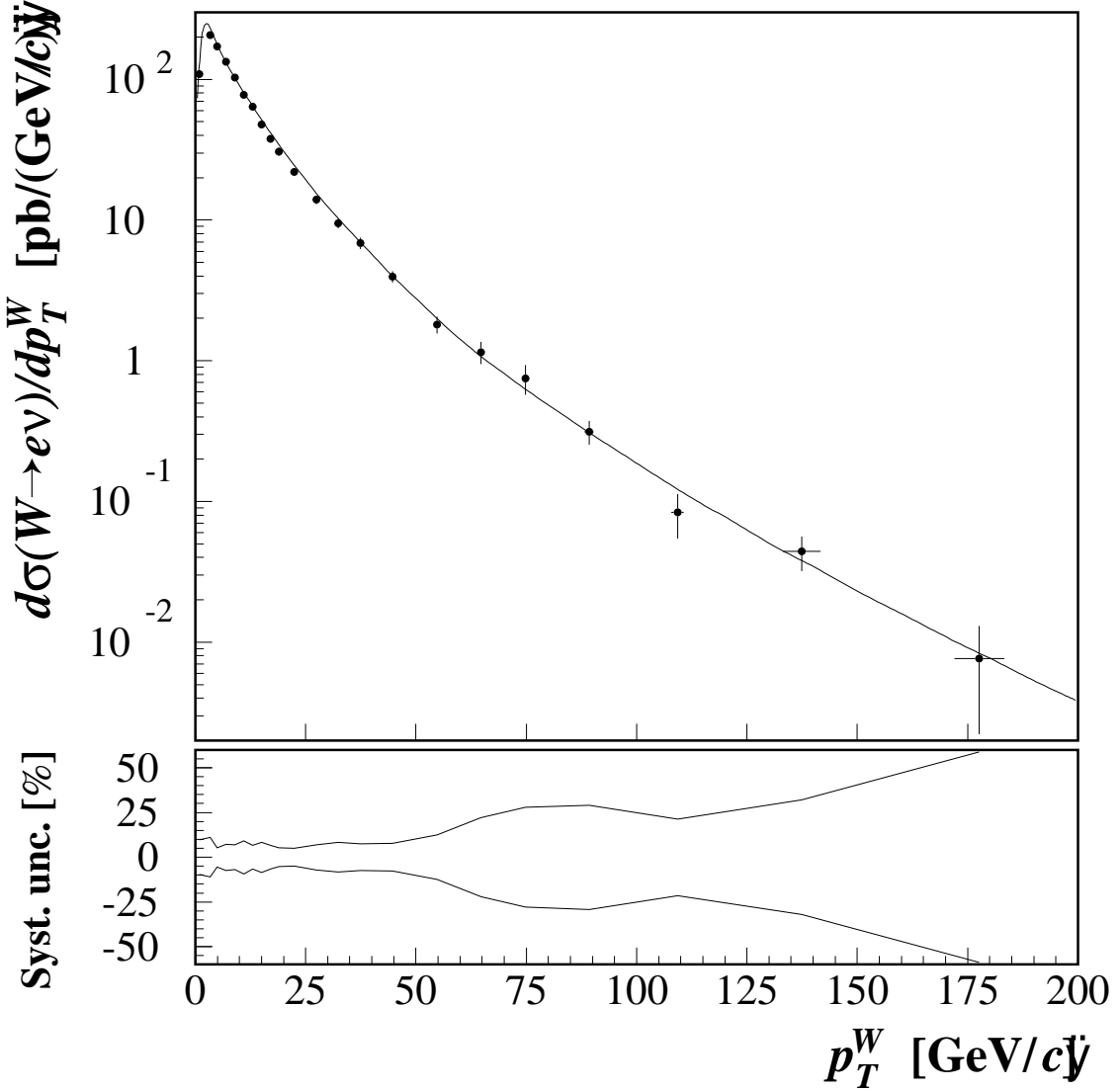


Fig. 1. Differential cross section for $W \rightarrow e\nu$ production. The solid line is the theoretical prediction of Ref. [6]. Data points show only statistical uncertainties. The fractional systematic uncertainty, shown as the band in the lower plot, does not include an overall 4.4% normalization uncertainty in integrated luminosity.

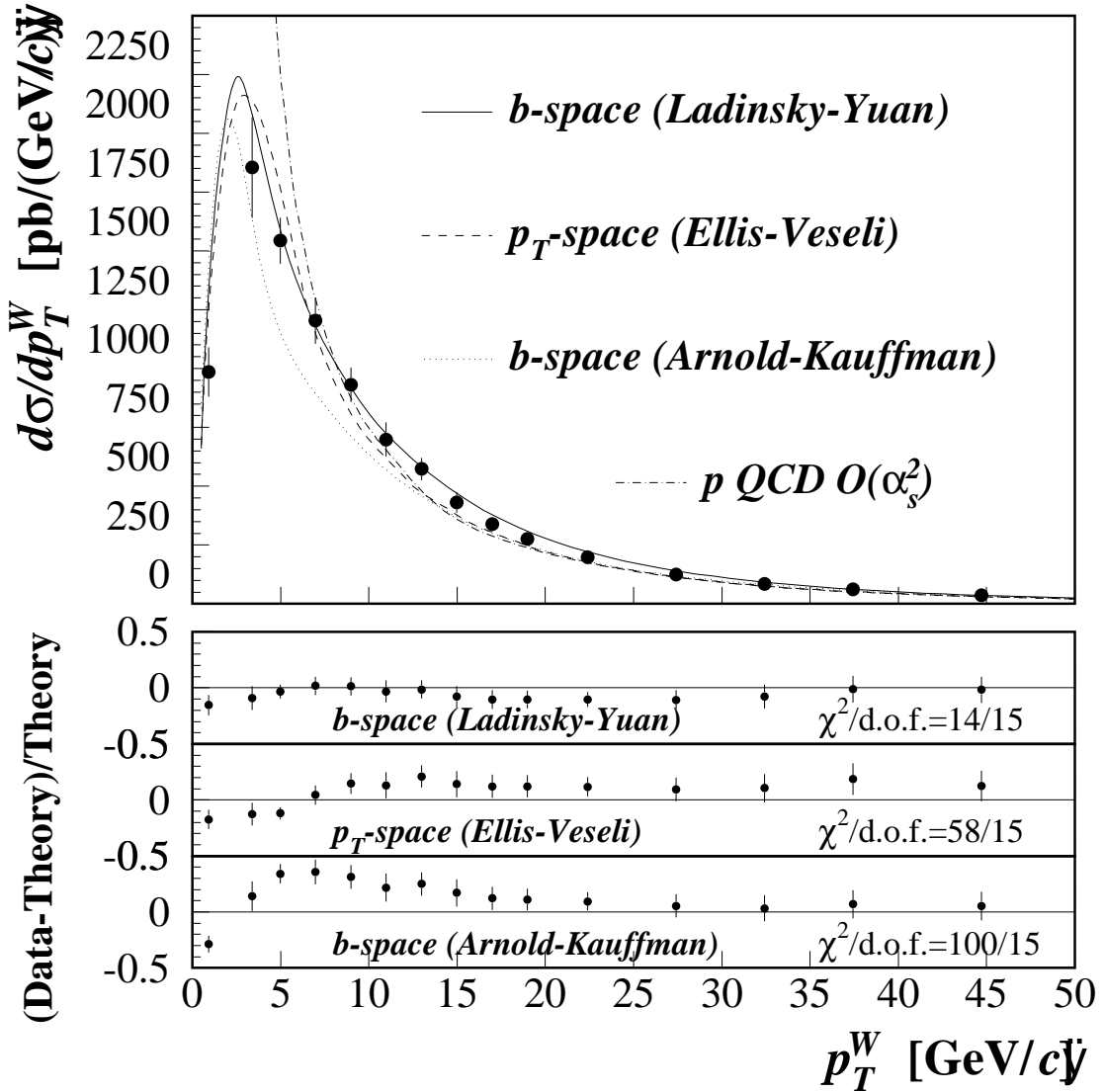


Fig. 2. Differential cross section for W boson production compared to three resummation calculations and to the fixed-order calculation. Uncertainties on data include both statistical and systematical contributions (other than an overall normalization uncertainty in integrated luminosity). Also shown are the fractional differences (Data–Theory)/Theory between data and the resummed predictions.

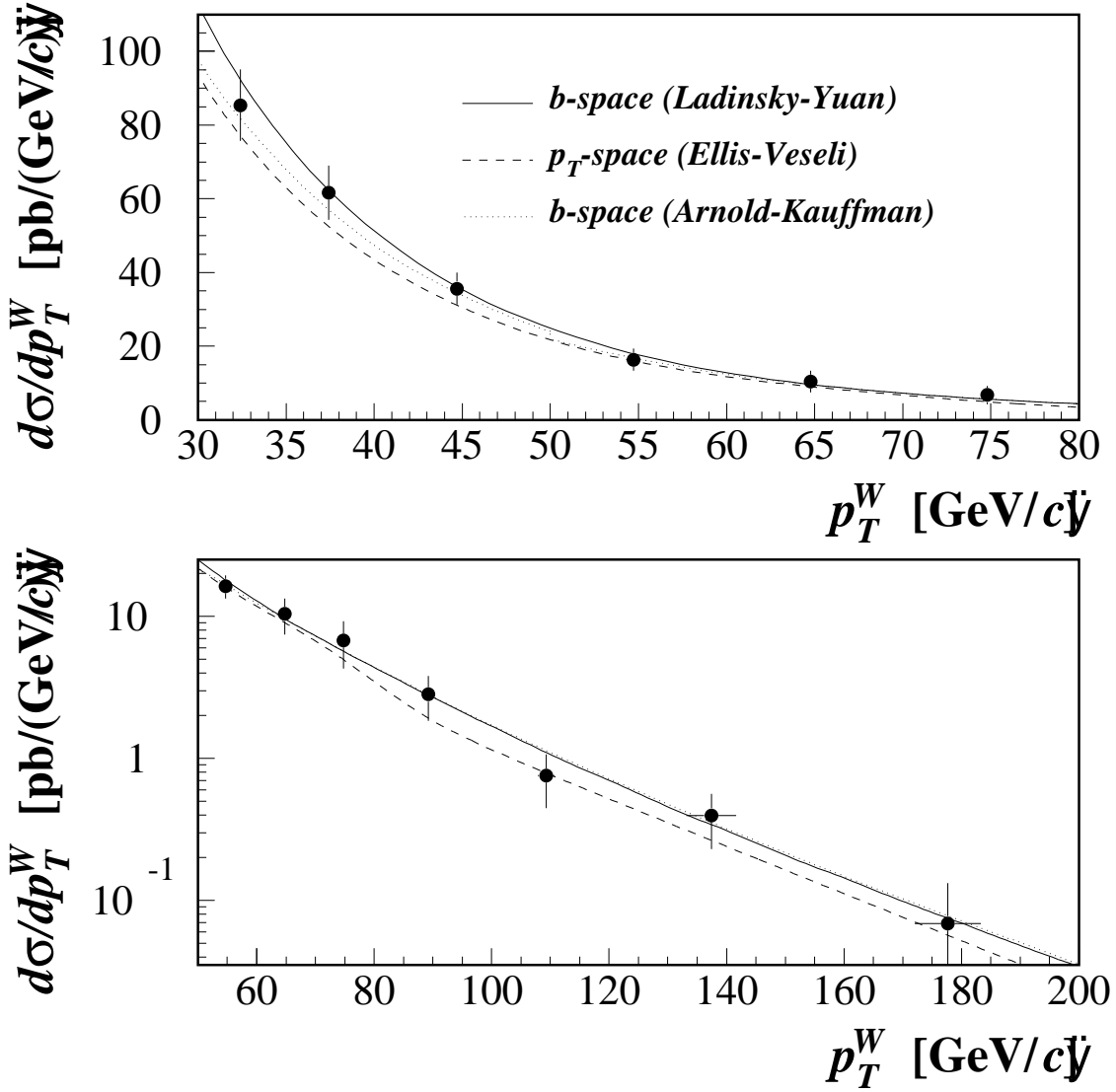


Fig. 3. Differential cross section for W boson production in the intermediate and high p_T^W regions. Uncertainties on data include both statistical and systematical contributions (other than an overall normalization uncertainty in integrated luminosity).